Available online at www.sciencedirect.com
SCIENCE DIRECT
Catalysis Today 116 (2006) 121–131
CATALYSIS TODAY
www.elsevier.com/locate/cattod

# In situ spectroscopic investigation of activation, start-up and deactivation of promoted sulfated zirconia catalysts

Barbara S. Klose [a], Friederike C. Jentoft [a,*], Pradnya Joshi [a], Annette Trunschke [a], Robert Schlögl [a], Irina R. Subbotina [b], Vladimir B. Kazansky [b]

[a] *Department of Inorganic Chemistry, Fritz Haber Institute of the Max Planck Society, Faradayweg 4-6, 14195 Berlin, Germany*
[b] *N.D. Zelinsky Institute of Organic Chemistry, Russian Academy of Sciences, Leninsky Prospect 47, Moscow 117913, Russia*

Available online 27 June 2006

**Abstract**

Sulfated zirconia (SZ), unpromoted and promoted with 0.5–2.0 wt.% Mn or Fe, was investigated by in situ IR and UV–vis spectroscopy during activation at 723–773 K and interaction with *n*-butane at 298–323 K. During start-up of the catalysts, the isomerization rate increases with the amount of water that is being formed, consistent with an activation of *n*-butane via oxidative dehydrogenation. Sulfate is the most likely oxidizing agent because activity is also observed for unpromoted SZ and without reduction of Mn. Isomerized species were also found on the surface of Fe-promoted SZ after exposure to *n*-butane without water formation indicating other yet unknown initiation pathways. During isomerization, Lewis acid sites on Fe-promoted SZ are blocked by water; the valence of Mn decreases only if the catalyst was previously activated in $O_2$. Stable species absorbing at 2820–2840 $cm^{-1}$ detected on the surface of SZ and Fe-promoted SZ after contact with *n*-butane at 298 K are tentatively ascribed to alkoxides, which may be side-products or intermediates. These species differ slightly for the two catalysts, reflecting the different structural and electronic properties of the materials.
© 2006 Elsevier B.V. All rights reserved.

*Keywords:* IR spectroscopy; UV–vis spectroscopy; Diffuse reflectance; In situ; Promoted sulfated zirconia; Butane isomerization; Catalyst deactivation

## 1. Introduction

Sulfated zirconia (SZ) is an attractive catalyst for low temperature alkane isomerization [1,2]. Its activity for butane conversion can be improved by 1–2 orders of magnitude through addition of iron or manganese cations, which exert a comparable promotional effect [3–6]. Initially SZ was believed to be a solid superacid [1] whose acidity could be further increased through promoters [7]. Except for the extraordinary catalytic activity and Hammett indicator methods [1], no other indications for superacidity were found. The alleged effect of the promoters on the acid strength originated from misleading data, and in fact most researchers could not find higher acid site strength or density after addition of Fe or Mn [8–10]. It was then proposed that promoters facilitate reaction initiation via oxidative dehydrogenation (ODH) to butenes, which may be converted into the reaction chain carriers, viz. carbenium ions. Evidence was indirect, such as better activity after activation in oxidizing rather than in inert atmospheres [11,12]. Iron (IV) oxy species were held responsible for the oxidation by Wan et al. [11]. Song and Kydd speculated that sulfate might provide the redox capability on SZ, which shows equal performance after activation in air or helium [12]. If differences exist in the initiation pathway for SZ and promoted SZ, they are not reflected in the product distributions obtained in the conversion of small hydrocarbons: with increasing temperature, skeletal isomerization, disproportionation, oligomerization and cracking products are observed for SZ and its promoted forms [2,13,14]. Promoted catalysts show higher activity at lower temperatures but activation energies for butane isomerization are similar; and Hsu et al. speculated that promotion increases the number of active sites rather than change their quality [3], consistent with the reports showing no increase in acid strength through promotion by Fe and Mn.

Lately, evidence has been accumulating that at least one pathway for butane activation on SZ catalysts is indeed ODH.

* Corresponding author. Tel.: +49 30 84134408; fax: +49 30 84134693.
*E-mail address:* jentoft@fhi-berlin.mpg.de (F.C. Jentoft).

0920-5861/$ – see front matter © 2006 Elsevier B.V. All rights reserved.
doi:10.1016/j.cattod.2006.01.036

Water has been detected by in situ IR spectroscopy, and the isomerization rate during the induction period has been found to be proportional to the amount of water formed [6,15]; this correlation applies for SZ and Mn-promoted SZ. During and after reaction at higher temperatures (423–573 K) unsaturated hydrocarbons were spectroscopically detected on the surface of SZ [16,17]; butene was inferred to desorb in TPD experiments [15]. The oxidizing agent in the unpromoted case appears to be sulfate; reduced S-containing species evolve, albeit at higher temperatures: at 673 K $SO_2$ [15] or at 523–573 K $H_2S$ [17,18]. Reduced S–O species, specifically dithionate, have only been detected on the surface of SZ after exposure of SZ to isobutyraldehyde [19]. For the promoted systems, reports on valence changes upon contact with feed differ: Millet et al. [20] reported reduction of Fe during reaction, while Mn was not reduced [21,22] or reduced in a way uncorrelated to performance [22].

According to the ODH hypothesis, isomerization on SZ materials would be initiated by a stoichiometric reaction. However, SZ may still act as a catalyst, because once the ''sites'' are activated, theoretically, an infinite number of turnovers is possible. It is assumed that upon contact with the feed, hydrocarbon surface species are formed via ODH and subsequent protonation. These species would be surface-equivalents of carbenium ions as exist in solutions and serve as chain carriers. Deactivation may occur if intermittently formed butenes polymerize on the surface or if isomerization or hydride transfer do not proceed properly and side products are formed. It has been proposed that water acts as a poison [23,24] or sulfate is lost, but once the site is activated this may not matter.

It is unresolved how the surface reactivity is related to the zirconia solid-state chemistry. Although sulfated monoclinic zirconia is catalytically active [25], the tetragonal phase is necessary for very good activity. On the other hand, not every tetragonal zirconia is highly active [26], indicating intrinsic variations in the phase are important. The promoters, Mn or Fe, are dissolved in the zirconia lattice and stabilize the tetragonal phase [5]. The fraction of surface and lattice promoter species depends on the promoter content and the preparation method, with Fe having a higher propensity to remain on the surface than Mn [5]. Solid solutions of Fe in zirconia were also inferred by Yamamoto et al. [21], Ohtsuka [27], and Xavier et al. [28]. These solid-state phenomena have yet to be connected to the performance.

The goal of this paper is to complete the picture on reaction initiation and deactivation for SZ in comparison to SZ promoted with Fe or Mn. We investigate the effect of the pretreatment atmosphere on Mn-promoted SZ by in situ UV–vis spectroscopy, measure the water accumulation during the start-up of butane isomerization on Fe-promoted sulfated zirconia by in situ IR spectroscopy, and describe surface hydrocarbon species formed during the reaction. Causes for deactivation are sought by in situ UV–vis spectroscopy and probing the sites after interruption of the reaction. In the discussion, we shall address similarities and differences between unpromoted and promoted SZ and possible relations between solid-state and surface chemistry in order to develop a unified model for all SZ catalysts.

## 2. Experimental

### 2.1. Catalyst preparation

Dried (21 h, 383 K) sulfated zirconium hydroxide (MEL Chemicals XZO 682/01) was used as precursor. Samples promoted with 0.5 or 2.0 wt.% iron or manganese (''0.5MnSZ'', ''2.0MnSZ'', ''2.0FeSZ'') were prepared from dried precursor according to the ''incipient wetness'' impregnation method, using aqueous solutions of either Fe(III) or Mn(II) nitrates (both Merck, p.a.), followed by drying for at least 24 h at room temperature. The raw materials were calcined in a 17.1 ml quartz boat under a 200 ml $min^{-1}$ synthetic air flow at 823 K (SZ) or 923 K for 3 h (3 K $min^{-1}$ nominal heating rate) [29,30].

### 2.2. UV–vis–NIR spectroscopy

Spectra were acquired in situ using a Perkin-Elmer Lambda 9 spectrophotometer, equipped with a Harrick Praying Mantis™ diffuse reflectance attachment type DRA-4-PE7 and a HVC-DR3 reaction chamber. About 160–200 mg of catalyst were supported on a stainless steel grid. The reflectance reference material was Spectralon® (UV–vis–NIR).

### 2.3. IR spectroscopy

In situ diffuse reflectance IR (DRIFT) spectra during *n*-butane adsorption and reaction were recorded with a Nicolet ''Impact 410'' FT-IR spectrometer using a mercury cadmium telluride (MCT) detector. A further development of the DRIFTS attachment described by Kazansky et al. [31], which uses only two mirrors to focus the IR beam onto the sample, was arranged in the beam path. The catalyst powder was pressed at 100 hPa for 2 s, sieved into fractions of 0.2–0.5 mm, and placed in a quartz cell equipped with a $CaF_2$ window. Samples touched the window, hence the beam path through the gas phase was limited to the void space within the catalyst bed, and gas phase contributions were minimized. The activation sequence consisted of drying in vacuum, oxidizing at 723 K, and finally evacuating at 773 K [17]. $CaF_2$ powder was used for background measurements. Spectra with 4 $cm^{-1}$ resolution were recorded at room temperature and processed with OMNIC™ software. For all spectra, the reflectance with respect to $CaF_2$ was converted into Kubelka–Munk units, setting the reflectance at 5000 $cm^{-1}$ to a value of 0.9.

In situ transmission IR spectra during isomerization and of adsorbed CO were acquired with a Perkin-Elmer System 2000 spectrometer, using a deuterated triglycine sulfate (DTGS) detector and Spectrum™ software. A high temperature cell ($T_{max}$ in beam 623 K [32]) with two $CaF_2$ windows connected to a vacuum and gas dosing system was placed in the sample compartment of the spectrometer. Powders were pressed into self-supporting wafers (20 s at 250 MPa) with a specific mass of 24–32 mg $cm^{-2}$. For activation, wafers were transferred within the closed system into a heatable section ($T_{max}$ = 823 K). CO was adsorbed on the activated catalyst and after *n*-butane

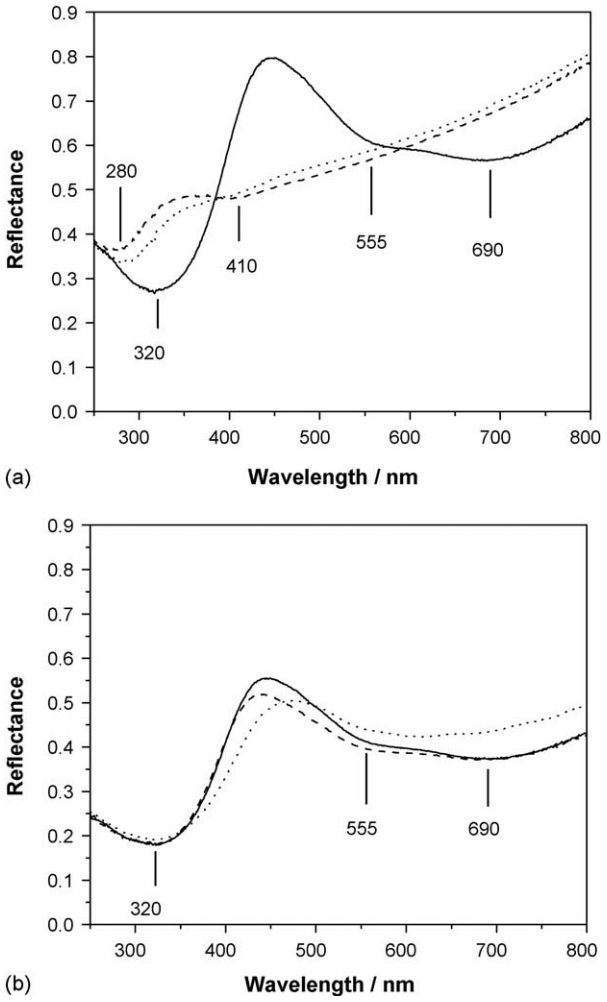


Fig. 1. UV–vis spectra of 0.5MnSZ before activation (solid line), at 773 K (dotted line), and after cooling to 323 K (dashed line): (a) in 20 ml $min^{-1}$ He; (b) in 20 ml $min^{-1}$ $O_2$.

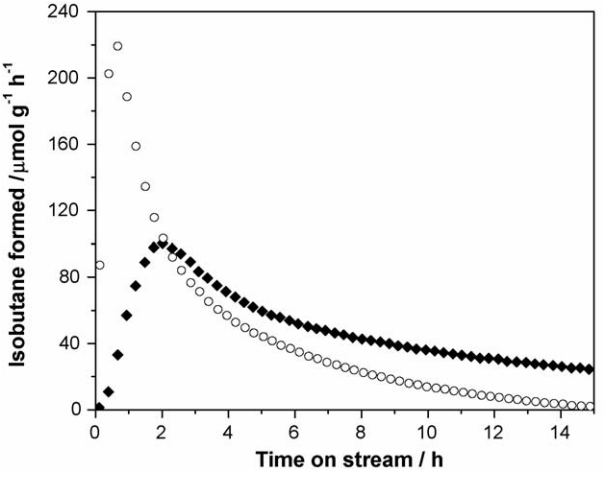


Fig. 2. Rate of *n*-butane isomerization vs. time on stream after activation in 20 ml $min^{-1}$ He (solid diamond) or $O_2$ (open circle). Conditions: 191 mg 0.5MnSZ (He activation) or 199 mg 0.5MnSZ ($O_2$ activation), 323 K, feed: 5% *n*-butane in $N_2$ (20 ml $min^{-1}$), activated at 773 K for 30 min (5 K $min^{-1}$ heating ramp).

isomerization. The reaction was stopped at different stages of catalytic activity by purging with $N_2$ until bands of butane were no longer detectable. The whole system was then evacuated by a turbomolecular pump (Pfeiffer, Balzers) for 1 h to a total pressure below $10^{-6}$ hPa before CO was dosed at room temperature via a variable leak valve (Varian). Spectra were converted into decadic absorbance.

### 2.4. Reaction conditions and product analysis

Catalytic experiments were conducted in flow at atmospheric pressure. Activation was carried out at nominal 723 K (transmission IR) or 773 K (UV–vis–NIR) in 20–40 ml $min^{-1}$ inert ($N_2$ or He) or oxidizing atmosphere. Reactions were conducted at 323 K at 1–5 kPa *n*-butane and flows between 20 and 30 ml $min^{-1}$. Product analysis for IR and UV–vis–NIR experiments was performed by on-line gas chromatography (Varian 3800, flame ionization detection).

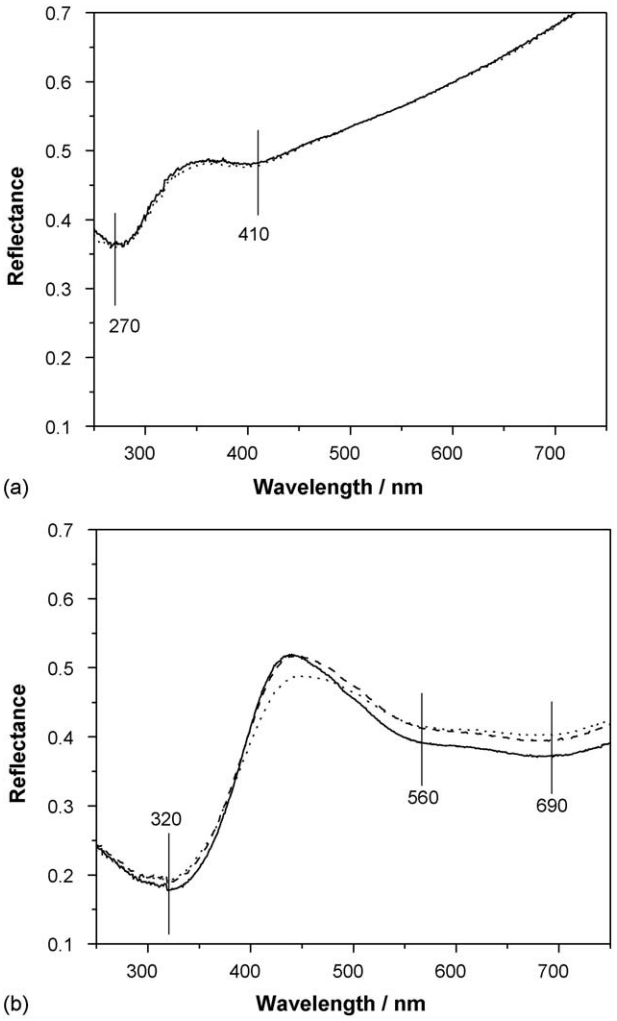


Fig. 3. UV–vis spectra of 0.5MnSZ recorded in situ before reaction (solid line), 7 h on stream (dashed line), or 15 h (dotted line) on stream: (a) previously activated in 20 ml $min^{-1}$ He; (b) previously activated in 20 ml $min^{-1}$ $O_2$. Conditions: 191 or 199 mg 0.5MnSZ, 323 K, feed: 5 kPa *n*-butane in balance of $N_2$ with total flow 20 ml $min^{-1}$, activated at 773 K for 30 min (5 K $min^{-1}$ heating ramp).

## 3. Results

### 3.1. UV–vis–NIR spectroscopy

The diffuse reflectance spectrum of calcined 0.5MnSZ shows a strong charge transfer band centered at 320 nm and at least two overlapping d–d transition bands at approximately 555 and 690 nm (Fig. 1). During activation in He, the bands at 320 and 690 nm lose intensity while absorption increases between 450 and 550 nm. The spectrum of the activated catalyst shows increasing absorption with increasing wavelength in the visible range and a small maximum at about 410 nm (Fig. 1a). During activation in $O_2$, the band at 690 nm decreases in intensity and is shifted towards the band at 555 nm. After cooling to reaction temperature (323 K) the spectrum resembles that measured before activation, except the band at 555 nm is more intense (Fig. 1b).

In the NIR region, bands at 1425 nm ≈ 7020 $cm^{-1}$ and 1920 nm ≈ 5210 $cm^{-1}$ arise from the overtone of the OH stretching vibration and a combination of OH stretching and deformation modes, respectively (not shown). These bands are diminished during the heat treatment, independent of the activation atmosphere.

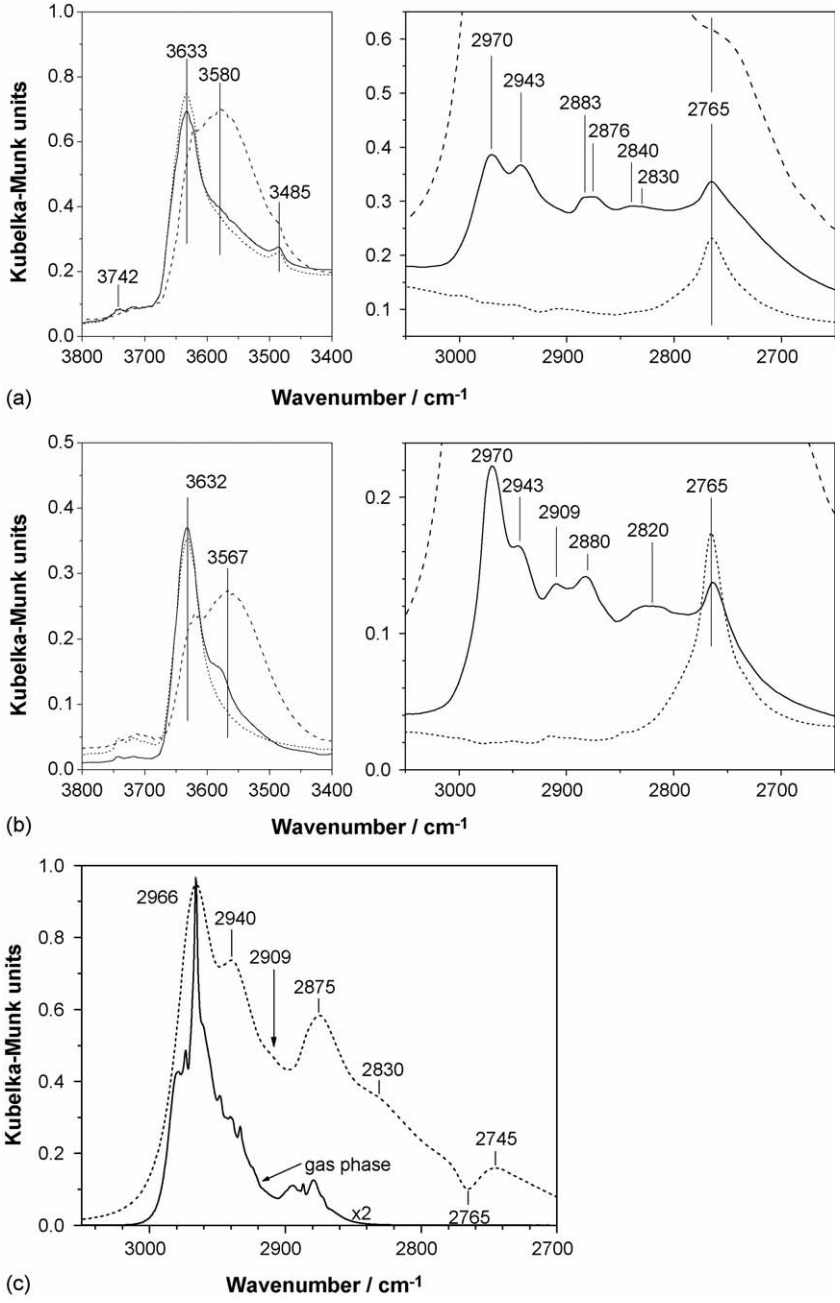


Fig. 4. DRIFT spectra recorded at room temperature: (a) SZ and (b) 2.0FeSZ after activation (dotted line), in presence of 100 hPa *n*-butane (dashed line) and after subsequent evacuation (solid line); (c) difference spectra of 12 hPa *n*-butane (dashed line) adsorbed on 2.0FeSZ recorded at room temperature (spectrum of activated 2.0FeSZ subtracted) and spectrum of gas phase *n*-butane (solid line).

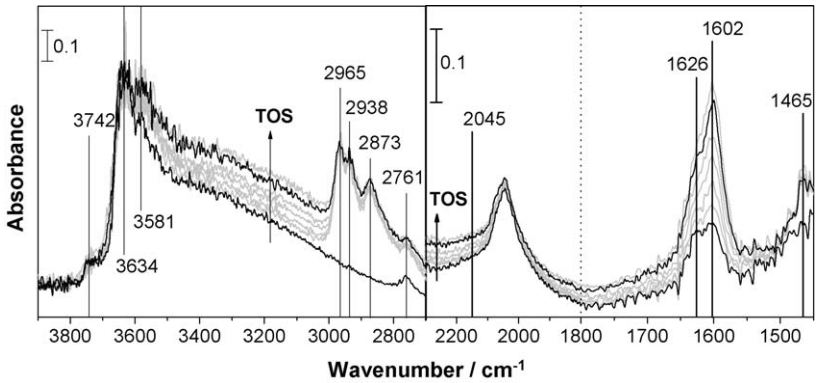


Fig. 5. FT-IR spectra of 2.0FeSZ taken in situ every 16 min during *n*-butane isomerization at 323 K (1 kPa *n*-butane in balance of $N_2$ with total flow 30 ml $min^{-1}$) after activation in 40 ml $min^{-1}$ $N_2$. Black: Spectra before start of reaction and at maximum rate.

Differently activated 0.5MnSZ samples were tested for *n*-butane isomerization; catalytic data corresponding to different activation procedures (Fig. 1) are shown in Fig. 2. All rate versus time-on-stream profiles are characterized by an induction period with increasing conversion until a maximum is reached. Activation in $O_2$ leads to a higher maximum conversion (ca. 220 μmol $g^{-1}$ $h^{-1}$, reached after 1 h) followed by a faster deactivation of the catalyst than activation in He (maximum conversion ca. 100 μmol $g^{-1}$ $h^{-1}$, reached after 2 h). The respective UV–vis spectra recorded in situ are shown in Fig. 3. For the catalyst that was activated in He (Fig. 3a), the spectrum taken after 15 h on stream does not differ from that taken before the start of reaction. After activation in $O_2$, the spectra of the 0.5MnSZ catalyst change during this period of time (Fig. 3b); a difference spectrum after conversion into Kubelka–Munk units reveals formation of a band at 410 nm and decreasing absorption at ca. 340 and 685 nm.

### 3.2. Diffuse reflectance infrared spectroscopy: n-butane adsorption and reaction

Fig. 4a and b show DRIFT spectra of SZ and 2.0FeSZ in the activated state in vacuum, during contact with 100 hPa *n*-butane

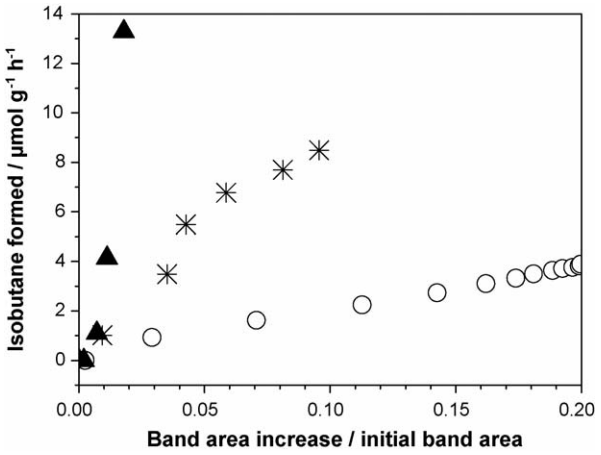


Fig. 6. Isobutane formation rate vs. area increase of water IR band centered at 1650–1600 $cm^{-1}$ during *n*-butane isomerization relative to the area of this feature before activation. 2.0FeSZ wafer in transmission (asterisk), 2.0MnSZ (solid triangle), and SZ powders (open circle) in diffuse reflection.

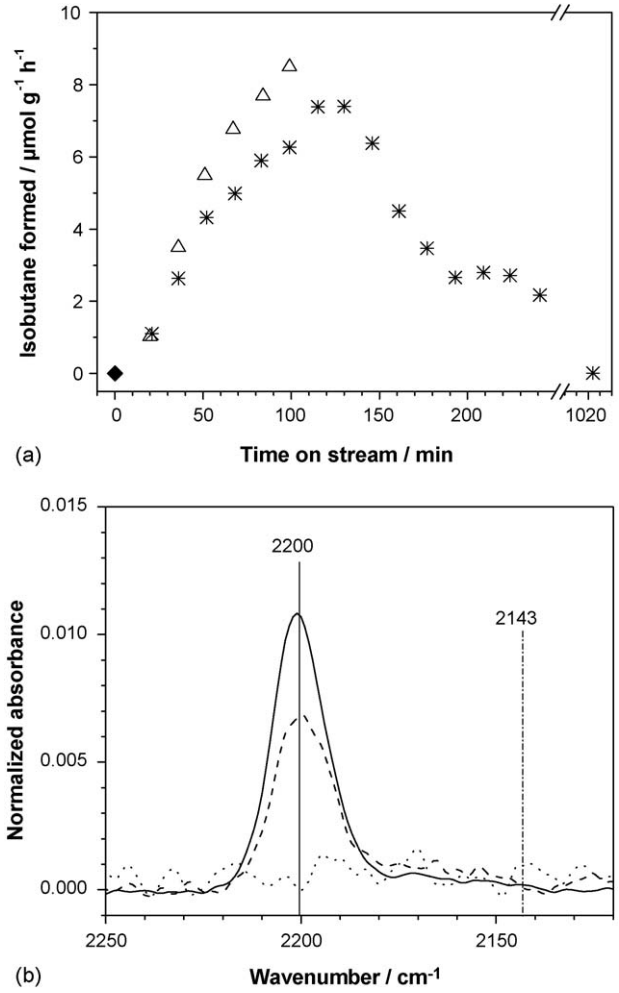


Fig. 7. (a) Rate of isomerization vs. time on stream of 2.0FeSZ at 323 K and total flow of 30 ml $min^{-1}$ of 1 kPa *n*-butane in balance of $N_2$ after activation in 40 ml $min^{-1}$ $N_2$ at 723 K; (b) FT-IR spectra of CO adsorption at RT after reaction was stopped, pressure 9 hPa CO. For each of the three experiments a fresh wafer was used, spectra are normalized to wafer area weight. Activated catalyst: solid line and solid diamond, stop after 100 min: dashed line and open triangle, stop after 17 h: dotted line and asterisk.

at room temperature, and after subsequent evacuation. In the OH stretching region, the band at about 3633 $cm^{-1}$ shifts to lower wavenumbers upon adsorption of *n*-butane for both catalysts. The additional band at 3485 $cm^{-1}$ of unpromoted SZ seems not to be affected. After evacuation, the spectra of SZ and 2.0FeSZ still exhibit bands in the CH stretching regime, and these adsorbate vibrations differ from those of the free butane molecule. The absorption around 2880 $cm^{-1}$ has a higher relative intensity than is typical for the butane gas, and for SZ is split into two bands at 2883 and 2876 $cm^{-1}$; this splitting was also observed at low butane coverages on 2.0FeSZ. For SZ, two bands that do not exist in the gas phase spectrum are observed at 2840 and 2830 $cm^{-1}$. Correspondingly, a broad absorption centered at 2820 $cm^{-1}$, consisting of more than one band, is detected for 2.0FeSZ. A band at 2909 $cm^{-1}$ is unique to the adsorbate on 2.0FeSZ. Also the shift of the OH-band is not completely reversible for 2.0FeSZ; however, insufficient evacuation cannot be excluded. Contact with butane does not result in a detectable increase of the absorption in the ranges 1600–1630 or 5225–5235 $cm^{-1}$ (SZ and 2.0FeSZ).

In an attempt to see if other, weakly adsorbed, species are detectable in presence of *n*-butane, but to avoid any interference of gas phase bands, spectra were recorded at only 12 h Pa. Fig. 4c shows a spectrum of *n*-butane adsorbed on 2.0FeSZ after subtraction of the spectrum of the activated catalyst in vacuum. The adsorbed state is characterized not only by a different pattern but also by broader bands in comparison to the narrow rotation-vibrational bands of gaseous butane (also shown). The intensity of the asymmetric $CH_3$ vibration at 2966 $cm^{-1}$ is decreased relative to the asymmetric $CH_2$ vibration at 2940 $cm^{-1}$. The corresponding symmetric CH vibrations appearing between 2885 and 2875 $cm^{-1}$ are more intense and red-shifted with respect to the gas phase feature at 2887 $cm^{-1}$. Furthermore, bands appear at 2909 $cm^{-1}$ (very weak) and 2830 $cm^{-1}$ (weak). The overtone of the S=O stretching vibration at 1402 $cm^{-1}$ is shifted from 2765 $cm^{-1}$ (negative band in difference spectrum) to 2745 $cm^{-1}$.

### 3.3. Transmission IR spectroscopy: n-butane reaction and CO adsorption

The 2.0FeSZ wafer prepared for transmission IR experiments is active for *n*-butane isomerization after activation in $N_2$ and shows a catalytic profile with a maximum in conversion after 1.5–2 h on stream. The IR spectra taken every 16 min during *n*-butane isomerization are displayed in Fig. 5; the spectrum at the start of the reaction and the spectrum corresponding to the maximum rate are shown in black. The OH stretching band around 3580 $cm^{-1}$ increases and C–H bands at 2965, 2938, 2873 $cm^{-1}$ (stretching modes), and 1465 $cm^{-1}$ (deformation mode) become visible as soon as the feed gas is admitted to the cell. OH deformation bands of adsorbed water at 1602 and 1626 $cm^{-1}$ increase with time on stream. For the S=O band at 1402 $cm^{-1}$ a shift towards lower wavenumbers and an intensity decrease are observed, while the S=O band at 1303 $cm^{-1}$ increases with time on stream (not shown).

The band area increase of the water feature including the bands at 1626 and 1602 $cm^{-1}$ of 2.0FeSZ (see Fig. 5) was determined from IR spectra by subtracting the area after activation from the area during the reaction. The simultaneously measured isobutane formation rate is plotted versus the band area increase in Fig. 6. To relate the transmission data of 2.0FeSZ to the results measured in diffuse reflectance using powder beds of 2.0MnSZ and unpromoted SZ [6], a reference point is needed. Before activation all calcined samples contain similar amounts of water, about 1.2–2.5 mmol $g^{-1}$ according to thermogravimetric measurements. Thus, the initial band area in the OH deformation region on all samples before activation should correspond to the same amount of adsorbed water, independent of the set-up. The relative water content during reaction is obtained by dividing the band area increase during reaction by the initial band area before activation. Fig. 6 suggests a linear correlation of rate and water content for all catalysts, whereby the isomerization rate increases from SZ $\ll$ 2.0FeSZ $<$ 2.0MnSZ for the same water content.

Adsorption of CO on 2.0FeSZ after activation in flowing $N_2$ was monitored by IR spectroscopy; difference spectra were created by subtracting the spectrum before from the spectrum after CO exposure. At low CO partial pressure only one band is visible at 2208 $cm^{-1}$. With increasing partial pressure the band increases in intensity and is red-shifted towards 2200 $cm^{-1}$. At very high partial pressure of ca. 200 hPa CO a second band appears at 2162 $cm^{-1}$. If 2.0FeSZ is activated in vacuum instead of in flowing $N_2$, a band at ca. 2160 $cm^{-1}$ forms already at a partial pressure of 5 hPa. The band increases in intensity and shifts to ca. 2155 $cm^{-1}$ with increasing CO pressure (not shown).

To determine the actually available sites on the surface of 2.0FeSZ during reaction, the reaction was interrupted at different stages, i.e. at maximum conversion or after many hours on stream, and CO was adsorbed. In Fig. 7a the catalytic data are displayed for three experiments with individual 2.0FeSZ wafers. The corresponding spectra in Fig. 7b at a partial pressure of 9 hPa show that the intensity of the CO band at 2200 $cm^{-1}$ decreases with time on stream.

## 4. Discussion

### 4.1. Catalyst activation

We have described DRIFT spectra of SZ, 2.0MnSZ, and 2.0FeSZ previously [6,17]. Several of the observed features are important for the discussion here. A strong decrease of the OH vibrations, especially of the characteristic combination of stretching and deformation modes of adsorbed water at around 5200 $cm^{-1}$ evidences dehydration during activation. The S=O stretching band located at ≈1400 $cm^{-1}$ after activation indicates $S_2O_7^{2-}$ according to DFT calculations [33]. The adsorbed-water content after activation in $N_2$-flow was about 60–125 μmol $H_2O$ $g^{-1}$. Variation of the activation atmosphere had little effect on the SO and OH vibrations of 2.0MnSZ. Strong Lewis acid sites capable of adsorbing $N_2$ at temperatures up to 358 K were found.

Before the transmission FT-IR measurements, 2.0FeSZ had to be pressed to form a self-supporting wafer, which can cause

phase transformation [34]. If 2.0FeSZ is pressed for 10 min at 540 MPa, a fraction of the metastable tetragonal phase is transformed, leading to 20–30 wt.% of the stable monoclinic form. In the experiments presented in this article, the wafer was pressed under less harsh conditions (20 s at 250 MPa) to minimize the phase transformation. Transmission spectra of 2.0FeSZ after activation (Fig. 5) confirm the results obtained by DRIFTS about the functional groups. The water loss of the 2.0FeSZ wafer during activation can be estimated from the decrease of the water deformation band at around 1600 $cm^{-1}$ and amounts to 96%, corresponding to a residual content of 45–93 μmol $H_2O$ $g^{-1}$, which is comparable to the results obtained in the DRIFTS cell.

The UV–vis spectra (Fig. 1) give additional information about the Mn species in the catalysts. XRD and ion scattering spectroscopy had revealed a large fraction of dissolved Mn in the zirconia lattice [5]; X-ray absorption fine structure (XAFS) analysis had yielded an average oxidation state in calcined 2.0MnSZ of 2.7–2.8 [22], suggesting mixed valences. The band at 320 nm can be assigned to a charge transfer from $O^{2-}$ to $Mn^{3+}$ [35], the band at 690 nm to a d–d transition of $Mn^{3+}$ [36]. A band around 555 nm has been attributed to a d–d transition of either $Mn^{2+}$ or $Mn^{3+}$ [37]. Even though $Mn^{2+}$ d–d transitions are spin-forbidden [13] and thus weak, such transitions should contribute because $Mn^{2+}$ is the only likely oxidation state in these catalysts that allows for an average valence <3. Hence, the Mn-promoted catalyst contains a mixture of $Mn^{3+}$ and $Mn^{2+}$ after calcination.

The Mn species are only slightly influenced by activation in oxidizing atmosphere (Fig. 1b). Activation in He (Fig. 1a) leads to a band at 410 nm, which is close to the absorption of $Mn^{2+}$ in an octahedral environment [38]. However, treatment of unpromoted SZ in inert gas also produces a (much weaker) band in this range (not shown), which has been assigned to a composite of absorptions by electron (F, $F^+$ and $Zr^{3+}$) and hole (V) color centers [39]. A band at 485 nm has been assigned to $Mn^{2+}$ in MnO [38], a band at 480 nm to $Mn^{3+}$ in $Mn_2O_3$ [35], i.e. changes in this range are ambiguous. Significantly weakened are the two bands at 320 and 690 nm, which are charge transfer and d–d transitions associated with $Mn^{3+}$. In summary, these spectral changes are in favor of partial reduction of Mn during pretreatment and are consistent with XAFS measurements, which indicate only a slight decrease in the average Mn valence from 2.77 to 2.72 after activation in 50% $O_2$ and a pronounced reduction of Mn to an average valence of 2.55 after activation in He [22]. Hence, after activation in different atmospheres the redox properties of the Mn-promoted catalyst should differ, while the functional groups such as sulfate and OH groups are in a comparable state [6].

### 4.2. Catalyst start-up and performance

In situ IR spectra of FeSZ (Fig. 5) reveal an increase of the OH deformation bands at 1602 and 1626 $cm^{-1}$ with time on stream, consistent with the formation of increasing amounts of water. More than one frequency may be observed because of water adsorption on different sites or, at higher degrees of hydration, due to association of water molecules [17]. For SZ and MnSZ, the rate of isomerization during the start-up has been found to be proportional to the area of the vibrational bands of water [6,15] and Fig. 6 demonstrates that this relationship also applies for FeSZ. The linear correlation between rate and number of water molecules is in favor of a reaction initiation via oxidative dehydrogenation of *n*-butane according to the following equation: oxidized catalyst + $C_4H_{10} \rightarrow C_4H_8 + H_2O$ + reduced catalyst. Assuming ODH, one molecule $H_2O$ is formed per reactive intermediate (carbenium ion generated via protonation of butene). If all $H_2O$ molecules stick to the catalyst (reaction temperature: 323 K), the number of adsorbed water molecules is proportional to the number of chain carriers and in turn, the rate of isomerization is proportional to the number of these reactive intermediates.

Fig. 6 reveals that for the same $H_2O$ deformation band-area increase the isomerization rate is not the same for 2.0MnSZ, 2.0FeSZ, and SZ. The differences between Mn- and Fe-promoted SZ may in part be ascribed to experimental circumstances: 2.0MnSZ was measured as a powder, 2.0FeSZ as a wafer. The observed lower rate of 2.0FeSZ may be due to mass transfer limitations in the wafer and partial monoclinization. However, the isobutane production per water molecule is much higher in the case of promoted catalysts. There are several potential reasons for this behavior: (i) assuming only a monomolecular mechanism, the actual turnover rate per site is higher, (ii) a higher site density favors the bimolecular mechanism with its lower activation energy [40] over the monomolecular mechanism, or (iii) there is another route to ''active sites'' (carbenium ions) without the formation of water, e.g. via protonation and cleavage of $H_2$, which, however, has only been demonstrated for unpromoted sulfated zirconia [41].

Given that ODH is a major route of initiation, one would expect a highly oxidized state of the catalyst to be advantageous in providing oxidation equivalents, and possibly a highly hydrated state to be disadvantageous, because a driving force for water formation could be the energy that is released upon its adsorption on coordinatively unsaturated (cus) sites. Indeed, for 0.5MnSZ, change of the activation atmosphere from inert to oxidizing leads to an increased activity followed by more rapid deactivation (Fig. 2). The higher activity after activation in $O_2$-containing atmosphere is consistent with our previous results obtained in a DRIFTS [6] or a XAFS [22] in situ cell, and with the observations of Wan et al. [11] and of Song and Kydd [12] for Fe,Mn-promoted SZ. Because the Mn valence is also higher after activation in $O_2$, one might want to attribute the increased activity to generation of a larger amount of reaction chain carriers via ODH with Mn as oxidizing agent. During the start-up period Mn should then be reduced in an extent that can be correlated with the achieved rate. The data (Fig. 3) contradict such a scenario: for the catalyst activated in $O_2$, a band characteristic for $Mn^{2+}$ evolves at 410 nm with time on stream, indicating reduction of Mn; but after activation in He, the spectra of the reduced catalyst do not change during 13 h on stream, while conversion to isobutane is undergoing dramatic changes (Fig. 2). Both observations are consistent with our

previous XAFS results [22]. Start-up of the reaction is obviously possible without reduction of Mn, nevertheless higher activity than that intrinsic to SZ is obtained. As proposed earlier [6,15], sulfate is a likely oxidizing agent. The activation atmosphere has been reported to not affect the performance of unpromoted SZ [12], suggesting that S-species are immune to reduction (or oxidation) under these conditions; however, $SO_2$ evolution during activation in He has been reported [15]. The effect on the promoted catalysts could be explained as follows: TPD experiments with various bases [11,42] and also test reactions with $H_2$ and butane [6] showed that promoters render sulfate more susceptible to reduction. During activation in inert gas, along with the Mn, a fraction (the most reactive fraction) of the sulfate might be reduced, diminishing the resulting activity. DRIFT spectra however show no significant differences after activation in different atmospheres [6]. Another effect that could contribute to the better performance after activation in oxidizing atmosphere is removal of ubiquitous carbon contaminations, making more sites available and enhancing the activity. This should also apply for unpromoted SZ, and, in contrast to literature reports, preliminary experiments in our laboratory suggest that SZ might be slightly more active after activation in $O_2$ than after activation in He [43].

No general statement can be made about the influence of the hydration state. Song and Kydd had found small amounts of water to have a positive, large amounts to have a negative effect on the performance of SZ [12]; best performance was reported for 200 μmol $g^{-1}$ [44]. González et al. inferred that a water concentration of 75 μmol $g^{-1}$ is optimal [45], while we found that small variations of the water content by 2.5–5%, clearly visible in IR spectra, did not affect the catalytic performance of 2.0MnSZ [6].

### 4.3. Adsorption sites and surface hydrocarbon species

The CO adsorption data demonstrate that the 2.0FeSZ catalyst surface provides Lewis sites. The band appearing at 2208 $cm^{-1}$ can be assigned to a stretching vibration of CO interacting with cus $Zr^{4+}$ sites; a band at the same position has been reported for monoclinic or partly tetragonal SZ [46,47]. Pinna et al. found the band of CO adsorbed on cus $Zr^{4+}$ on SZ to be shifted from 2200 to 2210 $cm^{-1}$ with the CO partial pressure decreasing from 133 hPa to 1.6 Pa [48]. Consistent with the literature [8–10], promotion does not increase the (Lewis) acid strength. We presume these cus $Zr^{4+}$ sites are responsible also for adsorption of $N_2$ at room temperature in 1 atm $N_2$, which we have reported earlier [6]. Because iron is not very well incorporated into the zirconia lattice but accumulates on the surface [5], CO could also interact with cus $Fe^{x+}$ species. CO at cus $Fe^{3+}$ has been reported to show bands at 2150, 2138 and 2124 $cm^{-1}$ for Fe-containing zirconia [49], while $Fe^{x+}$ ($x < 3$) was found to show a band at 2170 $cm^{-1}$ for Fe-promoted SZ [50]. The CO band appearing around 2160 $cm^{-1}$ at high partial pressure can thus be attributed to CO on Lewis acidic iron species.

Concerning interaction of 2.0FeSZ with butane, the data recorded on 2.0FeSZ in transmission in the catalytic flow experiment at 323 K agree quite well with the results of the room temperature adsorption measured with DRIFTS. The data quality in transmission is inferior in comparison to DRIFTS due to low transmittance of the SZ samples. In both cases, the OH band at ca. 3632–3634 $cm^{-1}$ is shifted, more so in the DRIFTS than in the transmission experiment (65 $cm^{-1}$ versus 53 $cm^{-1}$) because of the higher butane pressure (100 hPa versus 10 hPa). These results prove interaction of butane with OH groups, viz. Brønsted sites. At 100 hPa the shift is slightly larger for 2.0FeSZ than for SZ (53 $cm^{-1}$, Fig. 4a); however, the OH vibrations are much more intense for SZ and at equal partial pressure, the population of OH sites with butane might be lower for SZ, resulting in a shift comparable to that observed for 2.0FeSZ at lower partial pressure. The weak and upon evacuation mostly reversible shift is consistent with the low heats of alkane adsorption of 45–60 kJ $mol^{-1}$ measured for the majority of sites on these catalysts [26,51]. A red-shift of the S=O vibration as seen from the decrease of the band at 2765 $cm^{-1}$ and the concomitant appearance of a band at 2745 $cm^{-1}$ in the difference spectra (Fig. 4c) indicates interaction of butane not only with OH but also with sulfate groups.

The observed CH stretching vibrations in butane atmosphere also agree to a large extent in the DRIFTS and the transmission experiments performed using 2.0FeSZ. Stretching and deformation vibrations of *n*-butane can be seen at 2966, 2940, 2875 and 1466 $cm^{-1}$ (Fig. 4c) versus 2965, 2938, 2873, and 1465 $cm^{-1}$ (Fig. 5). These bands represent $\upsilon_{as}(CH_3)$, $\upsilon_{as}(CH_2)$, partially resolved $\upsilon_s(CH_3)$ and $\upsilon_s(CH_2)$, and $\delta(CH_3,CH_2)$ vibrations; the bands are broader and the symmetric stretching vibrations have a stronger relative intensity than in the gas phase butane spectrum. After removal of weakly adsorbed species by evacuation, a band at 2909 $cm^{-1}$ can be discerned in the DRIFT spectra of 2.0FeSZ. The frequency is characteristic of CH stretching vibrations of methyne groups, indicating the formation of isomerized species on the surface of 2.0FeSZ at room temperature. Such a band is not present for SZ, once more confirming the higher reactivity of promoted SZ at lower temperatures. Interestingly, no bands of water could be detected in the spectra of 2.0FeSZ in this room temperature batch experiment, suggesting that another channel of butane activation besides ODH may exist. Again, an additional mechanism would provide an explanation for a higher rate per formed water molecule for promoted compared to unpromoted SZ (Fig. 6); however, it is difficult to explain why the rate should still be roughly proportional to the amount of water formed.

Both the spectra of SZ and 2.0FeSZ exhibit further bands at 2820–2840 $cm^{-1}$. This frequency is close to that of CH vibrations in ethers, which lie below 2850 $cm^{-1}$. According to the supposed mechanism, isomerization of *n*-butane proceeds via carbenium ion type species [52–54]. Adsorbed carbenium ions can be expected to form ester or ether (alkoxide)-like structures with surface oxygen of the catalyst, analogous to solution chemistry [55]. The observed bands could represent such stable alkoxide species, which cannot desorb without hydride transfer from an incoming butane molecule or proton

elimination (at higher temperature?). Weakening of the symmetric CH stretching vibrations due to hydrogen bond formation is another possible explanation for these broad low frequency bands. These species absorb at 10–20 $cm^{-1}$ lower frequency on 2.0FeSZ than on SZ, indicating that at least a fraction experiences a different inductive effect by the bridge to the surface. Hence the electronic properties of the reactive surface sites are slightly different on these materials.

### 4.4. Catalyst deactivation

At different stages of catalytic activity, Lewis sites on the catalysts were probed by CO adsorption at room temperature (Fig. 7). At the same CO partial pressure of 9 hPa the band indicative of CO at Lewis sites is less intense after reaching the maximum rate than at the start of the reaction and has vanished after running the reaction for 17 h (Fig. 7). The capacity of 2.0FeSZ to adsorb CO on $Zr^{4+}$ Lewis sites decreases with time on stream and the amount of adsorbed CO can thus not be taken as a measure for the catalytic activity of 2.0FeSZ in the present state. CO is a poison that inhibits isobutane formation as long as it is added to the feed [48,56]; instead of blocking active Lewis sites that are necessary for isomerization [48], it is reacting with the adsorbed carbenium ions [56,57], so that their transformation to isobutane is hindered. Our adsorption experiments show that $Zr^{4+}$ sites that are able to interact with CO are blocked during *n*-butane isomerization. Either the reactant or its product or byproducts could be responsible for the consumption of Lewis sites. From the spectra recorded in situ during *n*-butane isomerization (Fig. 5), it is clear that water is formed. Because of its high electron density (free electron pairs) water is a much stronger Lewis base than alkanes. Thus, it is the water that adsorbs on 2.0FeSZ and blocks the Lewis sites. The activity increases while Lewis sites are already being blocked and decreases before all Lewis sites are covered with water (cf. Fig. 7a and b).

In the ODH activation scheme, one would expect the rate to level off once all active sites have reacted to produce water, a ''carbenium ion'' and a reduced catalyst site. Deactivation can only occur if any of the reaction steps during initiation, isomerization or hydride transfer does not proceed with 100% selectivity. The water formed during initiation adheres to the surface and could poison unreacted sites, but this should only lead to a lower maximum but not to a declining rate. Water can only be considered as a cause for deactivation, as inferred before [23,58], if it originates from other sources than ODH. We have previously found minor changes in the degree of hydration to have no effect on the catalytic performance [6].

The UV–vis spectra during isomerization over He-activated 0.5MnSZ reveal (Fig. 3a) that Mn is not reduced during reaction. The reduction observed after activation in $O_2$ occurs slowly and appears not related to the catalytic performance (Figs. 2 and 3b). These observations are consistent with previous results on the Mn valence in 2.0MnSZ obtained with in situ XAFS spectroscopy [22]. A slow dying-out of the isomerization, because of side reactions and the lack of redox-active promoter species to initiate new cycles as proposed by Wan et al. [11] or Millet et al. [20] for Fe-promoted material, is excluded for Mn. This observation supports the idea that the oxidizing species for ODH is sulfate.

The side reactions that are responsible for deactivation are likely those producing stable carbon-containing surface species. In earlier work on the *n*-butane isomerization in the presence of SZ, a band at about 295–305 nm was assigned to allylic cations [16,59,60] and taken as an indication of unsaturated hydrocarbon deposits, which deactivate the catalyst. No comparable band is formed during isomerization with 0.5MnSZ, independent of the preceding activation procedure (Fig. 3), raising the question as to why this catalyst deactivates so rapidly (Fig. 2). IR spectra of MnSZ deactivated at 323 K were obscured by hydrogen bonding in the CH range so that deposits could not be identified, even after purging the feed gas from the reaction cell [6]. Heating to 773 K resulted in distinct bands characteristic of unsaturated hydrocarbon surface species [6], indicating that irreversibly adsorbed species had been present after reaction. The data obtained here for SZ and FeSZ suggest that strongly held species generated at low temperatures are of saturated nature. In this sense, we can currently not distinguish whether the species absorbing at 2820–2840 $cm^{-1}$, tentatively assigned to alkoxides, are intermediates and reaction chain carriers or ''dead-end'' stable side products.

### 4.5. Solid-state chemistry and sites

Sulfated zirconia materials are superior for *n*-butane isomerization than are other sulfated oxides [61], and tetragonal zirconia is more active than monoclinic zirconia [25]. The support structure and electronic properties thus determine the reactivity of the sulfate and the properties of the adsorption sites and potentially of other ''assisting'' sites. Many cations have been identified as promoters for sulfated zirconia, e.g. ions of V, Cr, Mn, Fe, Co, Ni, Al, or Ga [2,4,62–66]. The product distributions are very similar for differently promoted catalysts [4] and seem to depend more on the conversion than on the nature of these cations. One explanation for this behavior could be that the action of the promoters is such that their individual chemistry is of secondary importance. All of these ions (can) have a lower valence than the $Zr^{4+}$, and ions of V, Cr, Mn, Fe, Co, Ni, and Al can be dissolved in the zirconia lattice [5,67]. A consequence of the incorporation of these aliovalent ions is stabilization and variation of the lattice constants of the tetragonal phase, and for charge balance, defects such as oxygen vacancies have to be generated. Such a scenario is depicted in Scheme 1. The changes in geometric and electronic structure in the zirconia bulk and near-surface regions that are caused by the promotion will affect the surface sites (''star'' in scheme, representing any type of site such as cus metal cation, OH group, or sulfate). Lewis and Brønsted acid strength sites were not significantly altered through the promotion (this work, [8–10,17]) but the reactivity of sulfate was found to be increased [17]. The fact that all promoters are similar in their influence on the catalytic behavior suggests that the dissolved species and the generated lattice defects (e.g. anion vacancies)

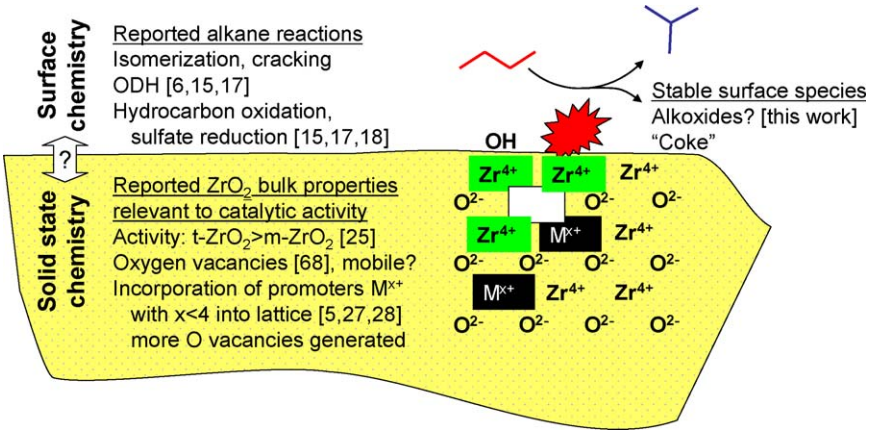


Scheme 1. Simplified representation of formation of active site. As so many zirconia bulk properties are relevant for the catalytic performance, it appears that the active site or an assisting site is connected to a specific feature of the bulk. $M^{x+}$: promoter or Zr with $x < 4$; (□): O vacancy; star: active site.

are responsible for the promotional effect and not surface promoter oxide species, which would be quite different in nature for the listed promoters. Further evidence for the importance of isolated promoter ions versus a promoter oxide phase is the fact that Mn is extremely well dispersed and incorporated and exerts a considerable effect already at a concentration as low as 0.5 wt.% [5,30]. Also, this model would explain the reactivity of unpromoted SZ if $M^{x+}$ in Scheme 1 is $Zr^{3+}$, i.e. the role of the promoter is taken over by $Zr^{3+}$. The concentration of $Zr^{3+}$ in a normal unpromoted SZ is presumably lower than a typical promoter concentration, resulting in fewer sites. The slight variations that result for different ions (e.g. $Fe^{3+}$ and $Zr^{3+}$) could be the reason for the different frequencies of the ''alkoxide'' species for SZ and Fe-promoted SZ. Further support for this model and the importance of oxygen vacancies can be summoned from the work of Vera et al. [68], who showed that partial reduction of the zirconia-support prior to addition of sulfate resulted in a more active catalyst.

### 4.6. Conclusions and outlook

Investigation of the amount of water on the surface of SZ, Mn-promoted SZ, and Fe-promoted SZ during *n*-butane isomerization gives a consistent picture [6, this work]: during the start-up of the catalyst, the isomerization rate increases with the amount of water that is being formed. This scenario is consistent with an activation of *n*-butane via ODH, which leads to the formation of a reaction chain carrier (''carbenium-ion-like''), water and a reduced catalyst species. Sulfate is the most likely oxidizing agent, because activity is observed for Mn-promoted SZ without reduction of Mn and also for unpromoted SZ. Activation in inert gas may have the disadvantage of reduction of a fraction of the most active sulfate [15] and will thus lead to a poorer performance than activation in an oxidizing atmosphere. This effect is more pronounced in the presence of promoters, which make the sulfate more susceptible to reduction [17]. Isomerized species were also found on the surface of Fe-promoted SZ after exposure to *n*-butane while water formation was not detected, and hence there seem to be other initiation pathways besides ODH, at least for this promoted catalyst.

Stable alkoxide-like species absorbing at 2820–2840 $cm^{-1}$ were detected on the surface of SZ and Fe-promoted SZ after contact with *n*-butane; it is not understood whether they are side-products or intermediates. The nature of these surface species was slightly different on the two catalysts, reflecting the different structural and electronic properties of the unpromoted and promoted SZ. It is suggested that near-surface defect states are generated by promoters ions dissolved in the zirconia lattice. These defects determine the support properties. This model would hold for many different promoters. In the future, this link between solid-state chemistry, i.e. the nature of the defects, and the surface chemistry will have to be elucidated.

## Acknowledgements

Barbara S. Klose, Annette Trunschke, and the cooperation between MPG and RAS were kindly supported by DFG grants JE 267/2-1 and 436 RUS 113/788/0-1. The authors thank Gisela Lorenz for assistance with the catalyst preparation, Carla Tschentscher and Heinz Junkes for developing the software to control the Lambda 9 spectrometer, and Rolf E. Jentoft for thermogravimetric measurements.

## References

[1] M. Hino, S. Kobayashi, K. Arata, J. Am. Chem. Soc. 101 (1979) 6439.
[2] M. Hino, K. Arata, J. Chem. Soc. Chem. Commun. (1980) 851.
[3] C.-Y. Hsu, C.R. Heimbuch, C.T. Armes, B.C. Gates, J. Chem. Soc. Chem. Commun. (1992) 1645.
[4] F.C. Lange, T.-K. Cheung, B.C. Gates, Catal. Lett. 41 (1996) 95.
[5] F.C. Jentoft, A. Hahn, J. Kröhnert, G. Lorenz, R.E. Jentoft, T. Ressler, U. Wild, R. Schlögl, C. Häßner, K. Köhler, J. Catal. 224 (2004) 124.
[6] B.S. Klose, F.C. Jentoft, R. Schlögl, J. Catal. 233 (2005) 68.
[7] C.-H. Lin, C.-Y. Hsu, J. Chem. Soc. Chem. Commun. (1992) 1479.
[8] V. Adeeva, J.W. de Haan, J. Jänchen, G.D. Lei, V. Schünemann, L.J.M. van de Ven, W.M.H. Sachtler, R.A. van Santen, J. Catal. 151 (1995) 364.
[9] J.E. Tábora, R.J. Davis, J. Chem. Soc. Faraday Trans. 91 (1995) 1825.
[10] R.S. Drago, N. Kob, J. Phys. Chem. B 101 (1997) 3360.
[11] K.T. Wan, C.B. Khouw, M.E. Davis, J. Catal. 158 (1996) 311.
[12] S.X. Song, R.A. Kydd, Catal. Lett. 51 (1998) 95.

[13] T.-K. Cheung, J.L. d'Itri, B.C. Gates, J. Catal. 151 (1995) 464.
[14] T.-K. Cheung, J.L. d'Itri, B.C. Gates, J. Catal. 153 (1995) 344.
[15] X. Li, K. Nagaoka, L.J. Simon, R. Olindo, J.A. Lercher, A. Hofmann, J. Sauer, J. Am. Chem. Soc. 127 (2005) 16159.
[16] R. Ahmad, J. Melsheimer, F.C. Jentoft, R. Schlögl, J. Catal. 218 (2003) 365.
[17] B.S. Klose, F.C. Jentoft, R. Schlögl, I.R. Subbotina, V.B. Kazansky, Langmuir 21 (2005) 10564.
[18] F.T.T. Ng, N. Horvát, Appl. Catal. A: Gen. 123 (1995) L197.
[19] M.V. Luzgin, K. Thomas, J. van Gestel, J.-P. Gilson, A.G. Stepanov, J. Catal. 223 (2004) 290.
[20] J.M.M. Millet, M. Signoretto, P. Bonville, Catal. Lett. 64 (2000) 135.
[21] T. Yamamoto, T. Tanaka, S. Takenaka, S. Yoshida, T. Onari, Y. Takahashi, T. Kosaka, S. Hasegawa, M. Kudo, J. Phys. Chem. B 103 (1999) 2385.
[22] R.E. Jentoft, A.H.P. Hahn, F.C. Jentoft, T. Ressler, Phys. Chem. Chem. Phys. 7 (2005) 2830.
[23] R.A. Comelli, C.R. Vera, J.M. Parera, J. Catal. 151 (1995) 96.
[24] C. Morterra, G. Cerrato, F. Pinna, M. Signoretto, G. Strukul, J. Catal. 149 (1994) 181.
[25] W. Stichert, F. Schüth, J. Catal. 174 (1998) 242.
[26] X. Li, K. Nagaoka, L.J. Simon, J.A. Lercher, S. Wrabetz, F.C. Jentoft, C. Breitkopf, S. Matysik, H. Papp, J. Catal. 230 (2005) 214.
[27] H. Ohtsuka, Catal. Lett. 90 (2003) 213.
[28] X. Carrier, P. Povilas, S. Kuba, L. Stievano, F.E. Wagner, M. Che, H. Knözinger, Chem. Phys. Chem. 5 (2004) 1191.
[29] A. Hahn, T. Ressler, R.E. Jentoft, F.C. Jentoft, Chem. Commun. (2001) 537.
[30] A.H.P. Hahn, R.E. Jentoft, T. Ressler, G. Weinberg, R. Schlögl, F.C. Jentoft, J. Catal. 236 (2005) 324.
[31] V.B. Kazansky, V.Yu. Borovkov, H.G. Karge, J. Chem. Soc. Faraday Trans. 93 (1997) 1843.
[32] H. Bludau, W. Nießen, H.G. Karge, Micropor. Mesopor. Mater. 22 (1998) 297.
[33] A. Hofmann, J. Sauer, J. Phys. Chem. B 108 (2004) 14652, personal communication.
[34] B.S. Klose, R.E. Jentoft, A. Hahn, T. Ressler, J. Kröhnert, S. Wrabetz, X. Yang, F.C. Jentoft, J. Catal. 217 (2003) 487.
[35] F. Milella, J.M. Gallardo-Amores, M. Baldi, G. Busca, J. Mater. Chem. 8 (1998) 2525.
[36] E. Fernández López, V. Sánchez Escribano, C. Resini, J.M. Gallardo-Amores, G. Busca, Appl. Catal. B: Environ. 29 (2001) 251.
[37] W. Sjoerd Kijlstra, E.K. Poels, A. Bliek, B.M. Weckhuysen, R.A. Schoonheydt, J. Phys. Chem. B 101 (1997) 309.
[38] G.W. Pratt Jr., Phys. Rev. 2 (1959) 281.
[39] A. Emeline, G.V. Kataeva, A.S. Litke, A.V. Rudakova, V.K. Ryabchuk, N. Serpone, Langmuir 14 (1998) 5011.
[40] H. Matsuhashi, H. Shibata, H. Nakamura, K. Arata, Appl. Catal. A: Gen. 187 (1999) 99.
[41] Z. Hong, K.B. Fogash, R.M. Watwe, B. Kim, B.I. Masqueda-Jiménez, M.A. Natal-Santiago, J.M. Hill, J.A. Dumesic, J. Catal. 178 (1998) 489.
[42] A. Jatia, C. Chang, J.D. MacLeod, T. Okubo, M.E. Davis, Catal. Lett. 25 (1994) 21.
[43] C. Chan Thaw, F. Garin, G. Tzolova-Müller, F.C. Jentoft, unpublished results.
[44] S.X. Song, R.A. Kydd, J. Chem. Soc. Faraday Trans. 94 (1998) 1333.
[45] M.R. González, J.M. Kobe, K.B. Fogash, J.A. Dumesic, J. Catal. 160 (1996) 290.
[46] V. Bolis, C. Morterra, B. Fubini, P. Ugliengo, E. Garrone, Langmuir 9 (1993) 1521.
[47] Z.T. Feng, W.S. Postula, C. Erkey, C.V. Philip, A. Akgerman, R.G. Anthony, J. Catal. 148 (1994) 84.
[48] F. Pinna, M. Signoretto, G. Strukul, G. Cerrato, C. Morterra, Catal. Lett. 26 (1994) 339.
[49] E. Guglielminotti, J. Phys. Chem. 98 (1994) 4884.
[50] C. Morterra, G. Cerrato, S. Di Ciero, M. Signorotto, A. Minesso, F. Pinna, G. Strukul, Catal. Lett. 49 (1997) 25.
[51] F.C. Jentoft, Habilitation Thesis, Humboldt-Universität zu Berlin, 2005.
[52] D.M. Brouwer, in: R., Prins, G.C.A., Schuit (Eds.), Chemistry and Chemical Engineering of Catalytic Processes, NATO ASI Ser. E, No. 39, Sijthoff and Noordhoff, Alphen aan den Rijn, The Netherlands, 1980, p. 137.
[53] G.A. Olah, Y. Halpern, J. Shen, Y.K. Mo, J. Am. Chem. Soc. 95 (1973) 4960.
[54] C.D. Nentitzescu, I.P. Cantuniari, Ber. Dtsch. Chem. Ges. 66 (1933) 10907.
[55] M.V. Frash, V.N. Solkan, V.B. Kazansky, J. Chem. Soc., Faraday Trans. 93 (1997) 515.
[56] S. Hammache, J.G. Goodwin Jr., J. Catal. 218 (2003) 258.
[57] V. Adeeva, H.-Y. Liu, B.-Q. Xu, W.M.H. Sachtler, Top. Catal. 6 (1998) 61.
[58] C. Morterra, G. Cerrato, F. Pinna, M. Signoretto, G. Strukul, J. Catal. 149 (1994) 181.
[59] F.R. Chen, G. Coudurier, J.-F. Joly, J.C. Védrine, J. Catal. 143 (1993) 616.
[60] D. Spielbauer, G.A.H. Mekhemer, E. Bosch, H. Knözinger, Catal. Lett. 36 (1996) 59.
[61] T. Yamaguchi, Appl. Catal. 61 (1990) 1.
[62] C. Miao, W. Hua, J. Chen, Z. Gao, Catal. Lett. 37 (1996) 187.
[63] M.A. Coelho, D.E. Resasco, E.C. Sikabwe, R.L. White, Catal. Lett. 32 (1995) 253.
[64] M. Signoretto, S. Melada, F. Pinna, S. Polizzi, G. Cerrato, C. Morterra, Micropor. Mesopor. Mater. 81 (2005) 19.
[65] Z. Gao, Y. Xia, W. Hua, C. Miao, Top. Catal. 6 (1998) 101.
[66] M. Perez-Luna, A. Cosultchi, J. Toledo-Antonio, E. Aree-Estrada, Catal. Lett. 102 (2005) 33.
[67] J. Stöcker, Ann. Chim. 5 (1960) 1459.
[68] C.R. Vera, C.L. Pieck, K. Shimizu, J.M. Parera, Appl. Catal. A: Gen. 230 (2002) 137.